Dynamic Surface Tension of Aqueous Surfactant Solutions. 6. Compounds Containing Two Hydrophilic Head Groups and Two or Three Hydrophobic Groups and Their Mixtures with Other Surfactants

Tao Gao and **Milton J. Rosen***
Surfactant Research Institute, Brooklyn College of CUNY, Brooklyn, New York 11210

Dynamic surface tensions (γ_t)—measured by the maximum bubble pressure method—of some surfactants containing two hydrophilic (sulfonate) groups and two or three hydrophobic groups in the molecule ("gemini surfactants"), and of their mixtures with a nonionic surfactant or an amine oxide, have been measured at 25°C in 0.1M NaCl. Linearity of the plots of surface pressure vs. square root of the surface age indicated that the systems studied were all diffusion-controlled. For the individual surfactant systems, the apparent diffusion coefficient decreases with an increase in the number of alkyl chains and the bulkiness of the surfactant molecules. For the mixtures, when interaction between the two surfactants is weak, γ_t at short times (t < 1s) is close to that of the component with the lower surface tension; at longer times, it is closer to that of the component with the lower equilibrium surface tension. When interaction is strong, γ_t at short times is greater than that of either component. The molar ratio at which maximum effect on γ_t is observed depends upon the strength of the interactions between the two surfactants.

KEY WORDS: Apparent diffusion coefficient, dynamic surface tension, gemini surfactants, maximum bubble pressure, surfactant interactions, surfactant mixtures, two hydrophilic groups.

In a previous paper (1), we reported that dynamic surface tension data, measured by the maximum bubble pressure method at a constant surfactant bulk concentration, can be represented by the following equation:

$$\gamma_t = \gamma_m + (\gamma_0 - \gamma_m)/[1 + (t/t^*)^n] \qquad [1]$$

where γ_t is the dynamic surface tension of the surfactant solution at time t, γ_m is the meso-equilibrium surface tension of the surfactant solution (where γ_t shows only a small change with time), γ_0 is the static (equilibrium) surface tension of the solvent, t* and n are constants depending on the nature of the surfactant and solution. Equation 1 can be transformed to the following logarithmic form:

$$\log[(\gamma_0 - \gamma_t)/(\gamma_t - \gamma_m)] = n \log t - n \log t^* \qquad [2]$$

From experimental data of γ_t and γ_m, values of t* and n can be calculated by using Equation 2 and the least-squares fitting method. It was reported (2) that the value of n increases with an increase in the hydrophobic character of the surfactant, and at a given Γ_{max}/C value, t* also increases with an increase in the hydrophobic character of the surfactant.

Hansen (3) has discussed the theory of diffusion-controlled adsorption for surfactants that obey the Langmuir adsorption isotherm (4):

$$\Gamma(C) = \Gamma_m bC/(1 + bC) \qquad [3]$$

where *b* is the Langmuir adsorption isotherm parameter (cm³/mole) relating the surface excess concentration $\Gamma(C)$, in mole/cm², to Γ_m, the maximum surface excess concentration, in mole/cm², and the bulk concentration C, in mole/cm³. The surface pressure, $\gamma_0 - \gamma$ can be related to the maximum surface excess concentration, Γ_m, and parameter *b* by the Szyszowski equation (5):

$$(\gamma_0 - \gamma)/\Gamma_m RT = \ln(1 + bC) \qquad [4]$$

Thus, the *b* value can be obtained by fitting Equation 4 to the equilibrium values of the surface tension as the function of bulk concentration by using the least-squares fitting method. The maximum surface excess concentration, Γ_m, can be calculated from the Gibbs adsorption equation (5). Then, the surface excess concentration $\Gamma(C)$ can be obtained from Equation 3 with the calculated values of *b*.

Bendure (6) has used Hansen's theory to derive equations for two limiting cases: (i) the initial (short-time) adsorption and (ii) the final (long-time) adsorption. For the short-time approximation, the equation is:

$$(\gamma_0 - \gamma_t)/C_0 = 2RT\,(D/\pi)^{1/2}t^{1/2} \qquad [5]$$

and for the long-time approximation:

$$\gamma_t - \gamma_e = \Gamma^2 RT/[C_0(\pi Dt)^{1/2}] \qquad [6]$$

where γ_0 and γ_t are the same as defined in Equation 1, in 10^{-5}N/cm (=mN/m); γ_e is the equilibrium surface tension of the surfactant solution, in 10^{-5}N/cm (=mN/m); Γ is the surface concentration at the aqueous solution/air interface, in mol/cm², calculated from Equation 3; C_0 is the bulk surfactant concentration, in mol/cm³, T is absolute temperature, in K°; D is the apparent diffusion coefficient of the surfactant, in cm²/s; and R is the gas constant, equal to 8.31 × 10²cm N/K° mol.

Equation 5 predicts that, at constant temperature, a plot of the reduced surface pressure (surface pressure divided by bulk concentration) as a function of the square root of the adsorption time should be linear, with a slope depending on the diffusion coefficient of the surfactant. In this paper we have measured dynamic surface tensions of some gemini anionic surfactants and of their binary mixtures with zwitterionic or nonionic surfactants. We have used Equations 2 and 5 to calculate values of n, t* and D for the individual surfactants, as well as for their mixtures, and we have investigated the effect of surfactant–surfactant interactions in binary mixtures containing gemini surfactants on these parameters and on the dynamic surface tension of the system.

---

*To whom correspondence should be addressed.

Copyright © 1994 by AOCS Press

MATERIALS AND METHODS

Materials. The chemical structures of the gemini compounds investigated are shown in Figure 1. Preparation and analysis have been reported previously—C_{10}DADS (7); $C_8C_1C_8$ and $C_8C_8C_8$ (8); $C_{10}OC_{10}$ and $C_{10}E_3C_{10}$ (9). Samples of $C_8C_1C_8$, $C_8C_8C_8$, $C_{10}OC_{10}$ and $C_{10}E_3C_{10}$ were obtained through the courtesy of Professors Y. Nakatsuji and A. Masuyama of Osaka University (Osaka, Japan). Polyoxyethylenated *n*-dodecyl alcohol with a homogeneous head group of seven oxyethylene units [$C_{12}(EO)_7$], purity > 98% by gas chromatography, was purchased from Nikko Chemicals Co. Ltd. (Tokyo, Japan). *N*, *N*-dimethyl-1-tetradecanamine oxide ($C_{14}N$) of > 95% purity was obtained from Ethyl Corporation (Baton Rouge, LA) courtesy of Kerry Hughes.

Equilibrium surface tension measurements. Equilibrium surface tension measurements were made by the Wilhelmy vertical-plate technique, with a sandblasted platinum blade of *ca.* 5-cm perimeter. The instrument was calibrated against quartz-condensed water each day that measurements were made. Sets of measurements were taken until the change in surface tension was less than 0.1 mN/m. Well-purified surfactants and their mixtures in the concentration range investigated here reached their equilibrium values in one hour or more. It usually takes several hours for dilute mixed surfactant solutions to reach the equilibrium value.

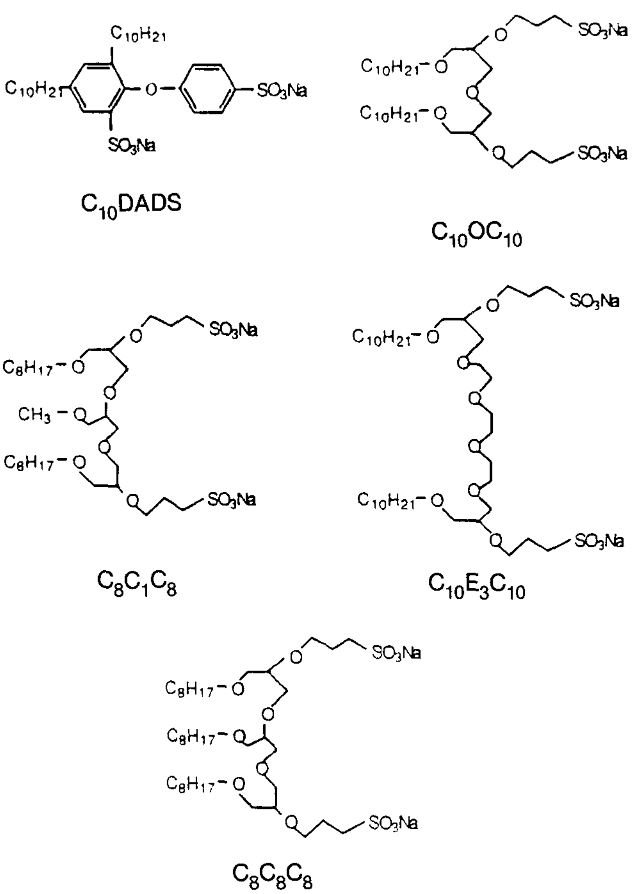

FIG. 1. Structures of gemini surfactants studied.

Dynamic surface tension measurements. The maximum bubble pressure method used in this work was described previously (1). All measurements were made at 25 ± 0.1°C.

RESULTS AND DISCUSSION

n and t values.* Plots of dynamic surface tension vs. log time for two gemini surfactants, C_{10}DADS and $C_8C_1C_8$, and a zwitterionic surfactant, $C_{14}N$, are shown in Figure 2; plots for $C_8C_8C_8$, $C_{10}E_3C_{10}$ and $C_{10}OC_{10}$ are given in Figure 3. Plots for the mixtures $C_8C_1C_8$–$C_{12}(EO)_7$, $C_8C_8C_8$–$C_{12}(EO)_7$, C_{10}DADS–$C_{12}(EO)_7$ and C_{10}DADS–$C_{14}N$ are shown in Figures 4, 5, 6, 7 and 8. The bulk concentrations for all these individual surfactants and the total bulk concentrations of the mixtures in Figures 4, 5, 6 and 7 are 1.0 × 10^{-3}M. The bulk concentrations in

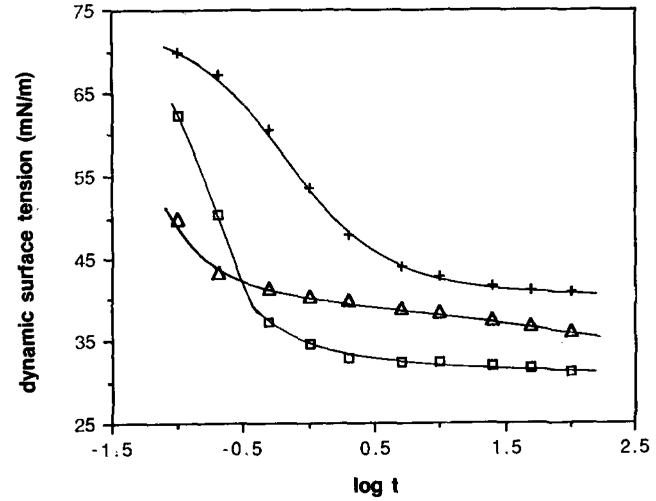

FIG. 2. Dynamic surface tension (γ_t) vs. log t plots for C_{10}DADS (+), $C_8C_1C_8$ (△), and $C_{14}N$ (□) in 0.1M NaCl at 25°C. The bulk surfactant concentrations for all surfactants are 1.0 × 10^{-3}M.

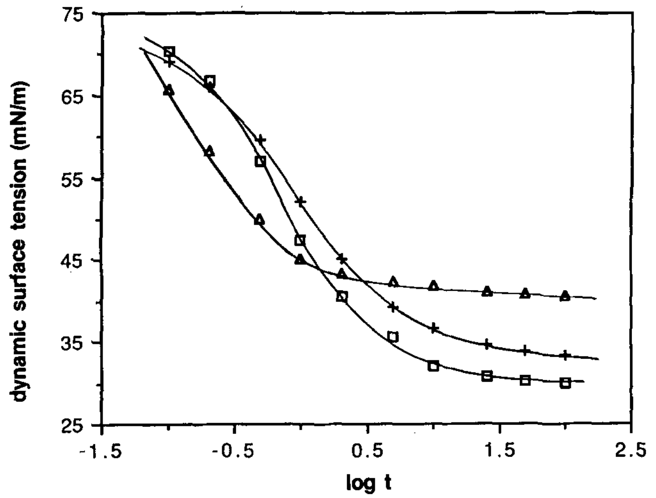

FIG. 3. Dynamic surface tension (γ_t) vs. log t plots for $C_8C_8C_8$ (□), $C_{10}E_3C_{10}$ (△) and $C_{10}OC_{10}$ (+) in 0.1M NaCl at 25°C. The bulk surfactant concentrations for all surfactants are 1.0 × 10^{-3}M.

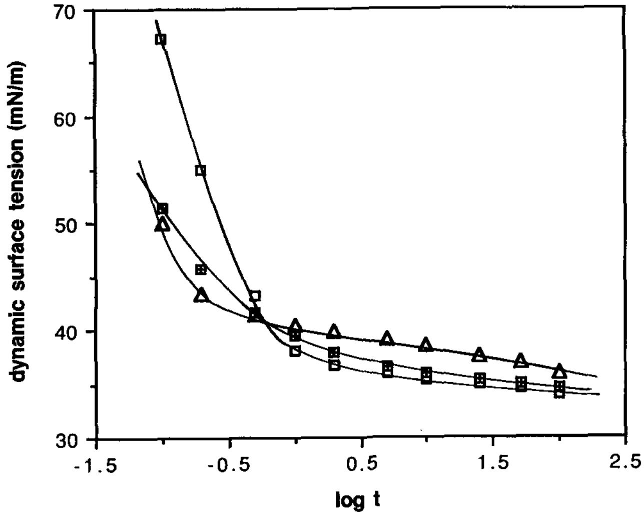

FIG. 4. Dynamic surface tension (γ_t) vs. log t plots for $C_8C_1C_8$ (△), $C_{12}(EO)_7$ (□) and their mixture $C_8C_1C_8$-$C_{12}(EO)_7$ (⊞) in 0.1M NaCl at 25°C. The bulk surfactant concentrations for individual surfactants and the total bulk concentration for the mixture are 1.0×10^{-3}M; $\alpha(C_8C_1C_8) = 0.60$.

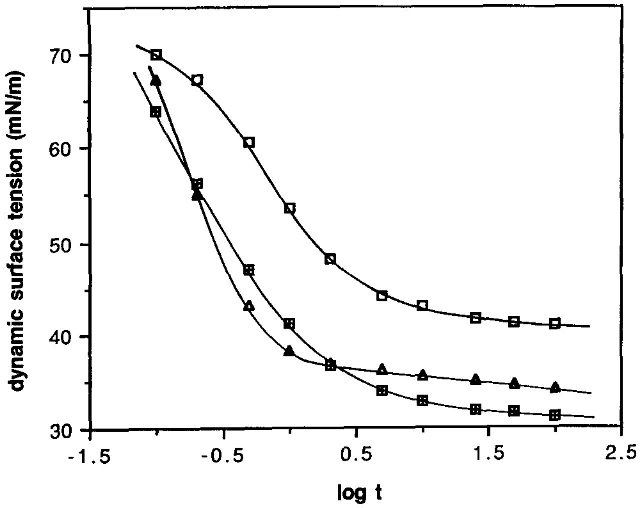

FIG. 6. Dynamic surface tension (γ_t) vs. log t plots for C_{10}DADS(□), $C_{12}(EO)_7$ (△) and their mixture C_{10}DADS-$C_{12}(EO)_7$(⊞) in 0.1M NaCl at 25°C. The bulk surfactant concentrations for the individual surfactants and the total bulk concentration for the mixture are 1.0 $\times 10^{-3}$M; $\alpha(C_{10}DADS) = 0.04$.

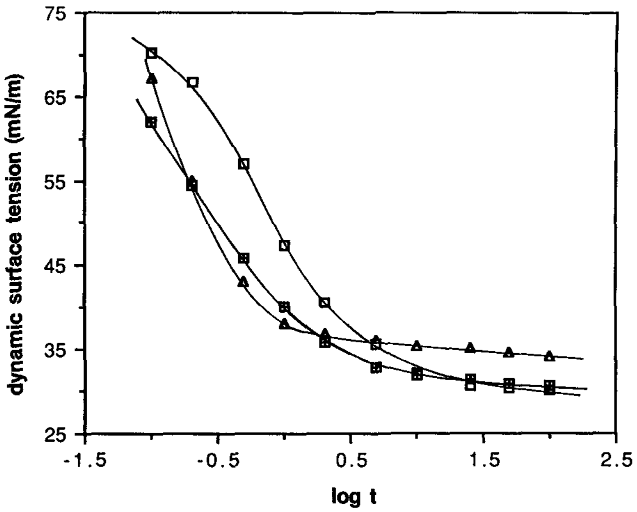

FIG. 5. Dynamic surface tension (γ_t) vs. log t plots for $C_8C_8C_8$ (□), $C_{12}(EO)_7$ (△) and their mixture $C_8C_8C_8$-$C_{12}(EO)_7$(⊞) in 0.1M NaCl at 25°C. The bulk surfactant concentrations for individual surfactants and the total bulk concentration for the mixture are 1.0×10^{-3}M. $\alpha(C_8C_8C_8) = 0.035$.

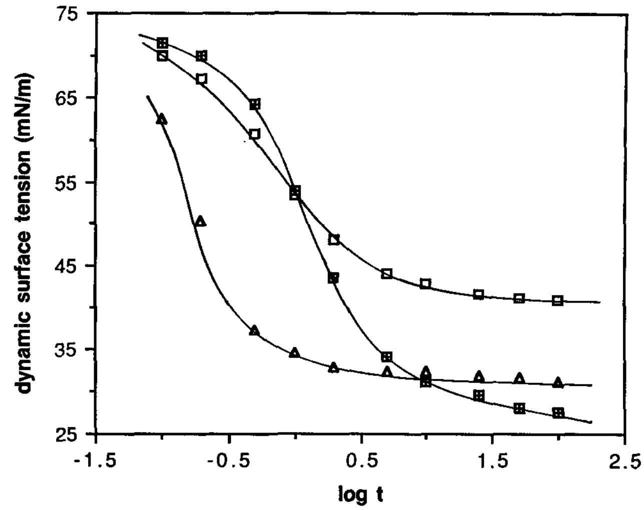

FIG. 7. Dynamic surface tension (γ_t) vs. log t plots for C_{10}DADS (□), C_{14}N (△) and their mixture C_{10}DADS-C_{14}N (⊞) in 0.1M NaCl at 25°C. The bulk surfactant concentrations for the individual surfactants and the total bulk concentration for the mixture are $1.0 \times$ 10^{-3}M; $\alpha(C_{10}DADS) = 0.35$.

Figure 8 for C_{10}DADS, C_{14}N and their mixture are 1.0×10^{-4}M. Plots of other surfactants and their mixtures at 1.0×10^{-4}M bulk concentrations have the same trends as shown in Figure 8 relative to Figure 7. The total ionic strength of all these surfactant solutions is kept constant at 0.1M NaCl. The calculated values of n and t* from Equation 2 for bulk surfactant concentrations 1.0×10^{-4}M and 1.0×10^{-3}M of investigated gemini and conventional surfactants in 0.1M NaCl aqueous solution are listed in Table 1.

Table 1 shows that the gemini surfactant with three alkyl chains ($C_8C_8C_8$) has the largest n value, and the gemini with most polyoxyethylene groups ($C_{10}E_3C_{10}$) has the lowest value of n. The value of n increases in the order: $C_{10}E_3C_{10} < C_{10}OC_{10} < C_8C_1C_8 < C_8C_8C_8$. This result is consistent with our previous conclusion (2) that the value of n increases with an increase in the hydrophobic character of the surfactant, and decreases with an increase in the length of the polyoxyethylene chains. Table 1 also shows that both n and t* decrease with an increase in bulk surfactant concentration, even though the bulk concentrations are above their critical micelle concentrations. This may indicate that the process of demicellization is fast compared to adsorption at the air/water interface. The calculated values of n and t* for mixtures containing gemini surfactants and C_{14}N or $C_{12}(EO)_7$ are listed in

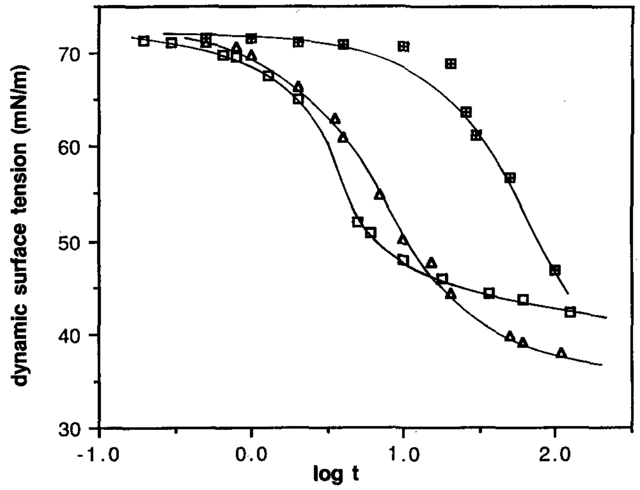

FIG. 8. Dynamic surface tension (γ_t) vs. log t plots for C_{10}DADS (□), C_{14}N (△) and their mixture C_{10}DADS-C_{14}N (⊞) in 0.1M NaCl at 25°C. The bulk surfactant concentrations for the individual surfactants and the total bulk concentration for the mixture are 1.0×10^{-4}M; $\alpha(C_{10}DADS) = 0.35$.

TABLE 1

Dynamic Surface Tension Parameters for Surfactants Investigated (0.1M NaCl, 25.0°C)

	C = 1.0 × 10^{-4} M		C = 1.0 × 10^{-3} M		
System	n	t* (s)	n	t* (s)	γ_{eq} (mN/m)
$C_{12}(EO)_7$	0.95	6.0	0.68	0.2	33.0
$C_{14}N(CH_3)_2O$	1.08	6.5	0.60	0.1	29.5
$C_{10}E_3C_{10}$	1.13	3.9	0.81	0.2	37.0
$C_{10}OC_{10}$	1.14	14.8	0.94	1.2	33.0
$C_8C_1C_8$	1.20	4.0	[a]	[a]	38.0
C_{10}DADS	1.28	4.4	0.92	1.0	39.8
$C_8C_8C_8$	1.59	9.0	1.00	1.1	29.0

[a] Plot of $\log[(\gamma_0-\gamma_t)/(\gamma_t-\gamma_m)]$ vs. log t is not linear.

TABLE 2

Dynamic Surface Tension Parameters for Mixtures Containing Gemini Surfactants (0.1M NaCl, 25.0°C)

		C = 1.0 × 10^{-4} M		C = 1.0 × 10^{-3} M	
System	α_1	n	t* (s)	n	t* (s)
$C_8C_1C_8$-$C_{12}(EO)_7$	0.600	0.98	6.2	0.42	0.03
$C_8C_8C_8$-$C_{12}(EO)_7$	0.035	1.13	7.1	0.80	0.3
C_{10}DADS-$C_{12}(EO)_7$	0.04	1.04	8.0	—	—
C_{10}DADS-$C_{12}(EO)_7$	0.10	1.12	8.0	—	—
C_{10}DADS-$C_{12}(EO)_7$	0.20	1.22	9.6	—	—
C_{10}DADS-$C_{12}(EO)_7$	0.35	1.24	14.5	—	—
C_{10}DADS-$C_{12}(EO)_7$	0.50	1.25	17.0	—	—
C_{10}DADS-$C_{12}(EO)_7$	0.80	1.16	8.8	—	—
C_{10}DADS-$C_{14}N(CH_3)_2O$	0.10	1.22	11.5	0.98	2.0
C_{10}DADS-$C_{14}N(CH_3)_2O$	0.20	1.23	18.5	1.00	2.2
C_{10}DADS-$C_{14}N(CH_3)_2O$	0.35	1.75	35.8	1.25	2.0
C_{10}DADS-$C_{14}N(CH_3)_2O$	0.50	1.66	32.1	1.05	1.9
C_{10}DADS-$C_{14}N(CH_3)_2O$	0.80	1.27	10.0	0.90	1.5

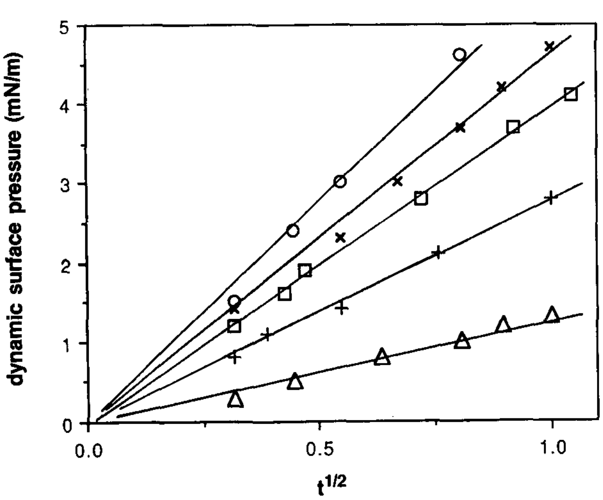

FIG. 9. Plots of surface pressure ($\gamma_0 - \gamma_t$) vs. the square root of time ($t^{1/2}$) for $C_8C_1C_8$ (X), $C_8C_8C_8$ (△), C_{10}DADS (O), $C_{10}OC_{10}$ (□) and $C_{10}E_3C_{10}$ (+) in 0.1M NaCl at 25°C at short time (t ⩽ 1 s). The bulk surfactant concentrations for all surfactants are 1.0×10^{-4}M.

Table 2. For C_{10}DADS–C_{14}N mixtures, n and t* increase with increasing α_1, the molar fraction of C_{10}DADS in the total bulk concentration of the mixed C_{10}DADS-C_{14}N surfactant solution, and reaches maximum values at $\alpha_1 = 0.35$. This may indicate the composition of the interaction product (see below).

Apparent diffusion coefficients (D). Plots of surface pressure ($\gamma_0 - \gamma_t$) vs. the square root of the time in seconds ($t^{1/2}$) for the compounds $C_8C_1C_8$, C_{10}DADS, $C_8C_8C_8$, $C_{10}OC_{10}$ and $C_{10}E_3C_{10}$ are shown in Figure 9. The values of the apparent diffusion coefficient D, calculated from Equation 5, for these gemini surfactants are listed in Table 3. The linearity of the plots and the values of D in the 10^{-6} cm²/s range indicate that adsorption is diffusion-controlled in these cases. The value of D increases in the order: $C_8C_8C_8 < C_{10}E_3C_{10} < C_{10}OC_{10} < C_8C_1C_8$.

It is apparent that the molecular size and shape play major roles in the diffusion-controlled adsorption. $C_8C_8C_8$, which has three alkyl chains in the molecule, should have the largest steric resistance in the diffusion process as compared to the other surfactants. $C_8C_1C_8$, which has two short chains in the molecule, should diffuse much faster than $C_8C_8C_8$. Comparing the structure of $C_{10}OC_{10}$ with that of $C_{10}E_3C_{10}$, the latter has three additional oxyethylene groups between the two alkyl chains in the molecule, so it should diffuse more slowly than $C_{10}OC_{10}$. The calculated D values are consistent with these considerations.

The D values for $C_{12}(EO)_7$, C_{14}N and their mixtures with various gemini surfactants are also listed in Table 3. It is noteworthy that the values for the $C_8C_1C_8$-$C_{12}(EO)_7$ and $C_8C_8C_8$-$C_{12}(EO)_7$ mixtures are not smaller than those of the components of the mixture, whereas for the C_{10}DADS-$C_{12}(EO)_7$, C_{10}DADS-C_{14}N and the $C_{10}E_3C_{10}$-C_{14}N mixtures, the D values are all significantly smaller than the value of either component.

Effect of strength of interaction between the two compounds on dynamic surface tension and apparent diffusion coefficient values. Interaction between the two components produces a complex with a greater molecular weight than either component. Consequently, this complex should have a smaller diffusion coefficient than either

TABLE 3

Calculated Values of Apparent Diffusion Coefficient (D) for Gemini Surfactants and Their Mixtures ($C = 1.0 \times 10^{-4}$ M, 0.1M NaCl, 25.0°C)

System	D
	($\times 10^6$ cm^2/s)
$C_8C_8C_8$	0.20
$C_{10}E_3C_{10}$	1.0
$C_{10}OC_{10}$	2.0
$C_8C_1C_8$	4.0
$C_{14}N(CH_3)_2O$	4.0
C_{10}DADS	4.2
$C_{12}(EO)_7$	6.8
$C_8C_8C_8$-$C_{12}(EO)_7$ ($\alpha_1 = 0.035$)	6.8
$C_8C_1C_8$-$C_{12}(EO)_7$ ($\alpha_1 = 0.600$)	4.0
C_{10}DADS-$C_{12}(EO)_7$ ($\alpha_1 = 0.04$)	3.4
C_{10}DADS-$C_{12}(EO)_7$ ($\alpha_1 = 0.10$)	3.1
C_{10}DADS-$C_{12}(EO)_7$ ($\alpha_1 = 0.20$)	1.5
C_{10}DADS-$C_{12}(EO)_7$ ($\alpha_1 = 0.35$)	2.0
C_{10}DADS-$C_{12}(EO)_7$ ($\alpha_1 = 0.50$)	3.3
C_{10}DADS-$C_{12}(EO)_7$ ($\alpha_1 = 0.80$)	1.7
C_{10}DADS-$C_{14}N(CH_3)_2O$ ($\alpha_1 = 0.35$)	0.05
$C_{10}E_3C_{10}$-$C_{14}N(CH_3)_2O$ ($\alpha_1 = 0.35$)	0.10

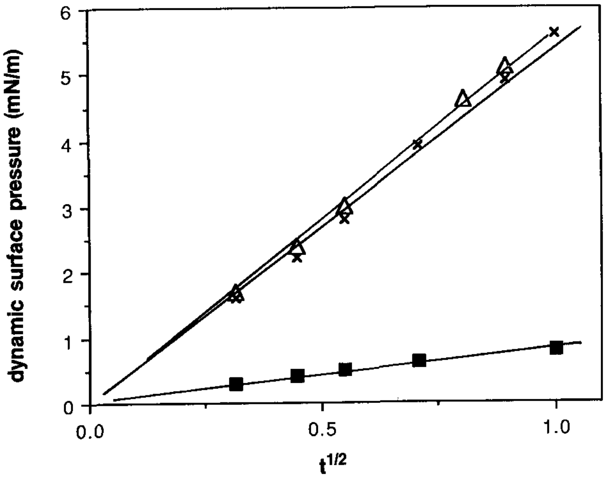

FIG. 10. Plots of surface pressure ($\gamma_0 - \gamma_t$) vs. the square root of time ($t^{1/2}$) for C_{10}DADS(X), C_{14}N (△) and their mixture C_{10}DADS-C_{14}N (■) in 0.1M NaCl at 25°C at short times ($t \leqslant 1$ s). The bulk surfactant concentrations for the individual surfactants and the total bulk concentration for the mixture are 1.0×10^{-4}M; α(C_{10} DADS) = 0.35.

component. We have previously reported (10) that geminis containing multiple ether oxygen atoms (for example, $C_8C_1C_8$ and $C_8C_8C_8$) have weaker interactions with polyoxyethylenated nonionic surfactants, such as $C_{12}(EO)_7$ ($\beta^\sigma = -1.5$ for $C_8C_1C_8$), than does C_{10}DADS ($\beta^\sigma = -5.9$), which has no multiple ether linkages, due to protonation of the ether oxygen atoms in the former gemini molecules. The larger D values listed in Table 3 for $C_8C_1C_8$ and $C_8C_8C_8$ mixtures with $C_{12}(EO)_7$, as compared to those of C_{10}DADS-$C_{12}(EO)_7$ mixtures, are consistent with this explanation. Figures 4, 5 and 6 show the differences in dynamic surface tension between mixtures $C_8C_1C_8$-$C_{12}(EO)_7$ or $C_8C_8C_8$-$C_{12}(EO)_7$ and mixture C_{10}DADS-$C_{12}(EO)_7$. In Figure 4, at short times ($\log t < 0$) the curve for the mixture $C_8C_1C_8$-$C_{12}(EO)_7$ is close to the curve of the individual surfactant ($C_8C_1C_8$) that has the lower surface tension. At longer times, the curve for the mixture follows the curve of the individual surfactant [$C_{12}(EO)_7$] that has the lower surface tension. Apparently there is no strong interaction between the two components of the mixture. In Figure 5, the same trend is observed for the mixture $C_8C_8C_8$-$C_{12}(EO)_7$. A different pattern is seen in Figure 6. At short times ($\log t < 0$), the curve for the mixture C_{10}DADS-$C_{12}(EO)_7$ is again close to the component [$C_{12}(EO)_7$] that has the lower surface tension, but at longer times, the curve for the mixture is below either curve for the individual components. This indicates that there is significant interaction in this mixture and that, at long times, the synergism in surface tension reduction effectiveness (i.e., lower equilibrium surface tension of the mixture, as compared to its components) shown by this mixture (11) determines the dynamic surface tension value.

As previously reported (10), C_{10}DADS has a stronger interaction with the zwitterionic surfactant C_{14}N ($\beta^\sigma = -7.3$) than with $C_{12}(EO)_7$ ($\beta^\sigma = -5.9$). Figures 7 and 8 show how this strong interaction between the two components affects the dynamic surface tension of the mixture C_{10}DADS-C_{14}N. In Figure 7, the total bulk concentration is again 1.0×10^{-3}M for both the individual surfactants and their mixture, and the mole fraction (α) of C_{10}DADS is 0.35 (approximately a 1:2 molar ratio of the divalent anionic to the zwitterionic). The dynamic surface tension for the mixture is greater than that of either component surfactant at short times ($t < 1$ s) and lower than that of either component at long times. This indicates formation of a complex with a slower diffusion rate than either component, but with a lower equilibrium surface tension (11). When the total bulk concentration is dereased to 1.0×10^{-4}M (Fig. 8), the short-time effect is even more apparent. Here, the period during which the dynamic surface tension value of the mixture is greater than that of either component extends to more than 100 s. Figure 10 shows the plots of dynamic surface pressure vs. square root of the time at short times ($t < 1$ s) for the individual components C_{10}DADS, C_{14}N and their mixture, C_{10}DADS-C_{14}N. The slope for the mixture is much smaller than that of either component. The calculated value of the apparent diffusion coefficient D for the mixture C_{10}DADS-C_{14}N, 5×10^{-8}cm^2/s, is about two orders of magnitude smaller than that ($\approx 4.0 \times 10^{-6}$ cm^2/s) for components C_{10}DADS and C_{14}N.

Effect of molar ratio of the two components. Changes in dynamic surface tension with time at different molar ratios of the components in C_{10}DADS-C_{14}N mixtures at total bulk concentrations of 1.0×10^{-4}M and 1.0×10^{-3}M in aqueous 0.1M NaCl are shown in Figures 11 and 12, respectively. The major effects of the interaction of the components (highest surface tensions at short times and lowest surface tensions at long times) are seen at $=\alpha_{C_{10}DADS} = 0.35$, a 1:2 molar ratio of the divalent anionic to the zwitterionic. The n values for these mixtures in Table 2 also show a maximum at $=\alpha_{C_{10}DADS} = 0.35$. This implies a structure for the interaction product involving one molecule of the disulfonated dialkyldiphenylether associated with two molecules of the

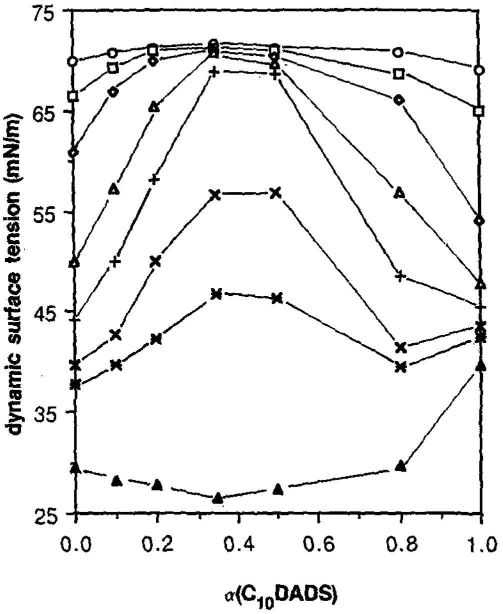

FIG. 11. Dynamic surface tension vs. molar ratio (α) of component C_{10}DADS in the total bulk concentration of the mixture C_{10}DADS-C_{14}N at different times. ○, 1 s; □, 2 s; = ◇ 4 s; △, 10 s; +, 20 s; X, 50 s; *, 100 s; ▲, equilibrium surface tension. The total bulk concentration is 1.0 × 10^{-4}M in 0.1M NaCl at 25°C.

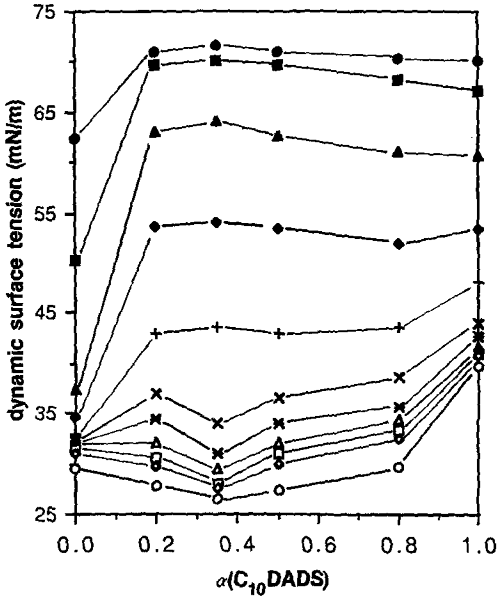

FIG. 12. Dynamic surface tension vs. molar ratio (α) of component C_{10}DADS in the total bulk concentration of the mixture C_{10}DADS-C_{14}N at different times. ●, 0.1 s; ■, 0.2 s; ▲, 0.5 s; ◆ , 1 s; +, 2 s; X, 5 s; *, 10 s; △, 25 s; □, 50 s; ◇ , 100 s; ○, equilibrium surface tension. The total bulk concentration is 1.0 × 10^{-3}M in 0.1M NaCl at 25°C.

protonated amine oxide. For the more weakly interacting C_{10}DADS-$C_{12}(EO)_7$ system, the n and t* values, shown in Table 2, reach a maximum value at $\alpha = 0.50$, indicative of a predominately 1:1 molar ratio. It appears that with increased strength of the interaction of the two components, the interaction product tends toward the 2:1 ratio, producing a complete mutual neutralization of the electrical charges in the two components.

ACKNOWLEDGEMENTS

This material is based upon work supported by the National Science Foundation (Grant CTS-9312715), the Colgate-Palmolive Company, Rhône-Poulenc Surfactants and Specialties LP and Witco Corporation.

REFERENCES

1. Hua, X.Y. and M.J. Rosen, *J. Colloid Interface Sci. 124*:652 (1988).
2. Hua, X.Y. and M.J. Rosen, *Ibid. 141*:180 (1991).
3. Hansen, R.S., *J. Phys. Chem. 64*:637 (1960).
4. Langmuir, I., *J. Am. Chem. Soc. 40*:1361 (1918).
5. Rosen, M.J., *Surfactants and Interfacial Phenomena*, 2nd edn., John Wiley & Sons, Inc., New York, 1989, pp. 68, 84.
6. Bendure, R.L., *J. Colloid Interface Sci. 35*:238 (1971).
7. Rosen, M.J., Z.H. Zhu and X.Y. Hua, *J. Am. Oil Chem. Soc. 69*:30 (1992).
8. Zhu, Y.P., A. Masuyama, Y.I. Kirito, M. Okahara and M.J. Rosen, *Ibid. 69*:626 (1992).
9. Zhu, Y.P., A. Masuyama, T. Nagata and M. Okahara, *J. Jpn. Oil Chem. Soc. 40*:473 (1991).
10. Rosen, M.J., Z.H. Zhu and T. Gao, *J. Colloid Interface Sci. 157*:254 (1993).
11. Rosen, M.J., T. Gao, Y. Nakatsuji and A. Masuyama, *Colloids and Surfaces*, in press (1994).

[Received December 14, 1993; accepted April 21, 1994]